CDF/PUB/BOTTOM/PUBLIC/10286

Measurement of the Bottom Baryon Resonances Σ_b and Σ_b^*

The CDF Collaboration
URL http://www-cdf.fnal.gov
(Dated: October 14, 2010)

Abstract

We present measurements of the masses and widths of the four states $\Sigma_b^{(*)\pm}$ in decays to $\Lambda_b^0\pi^\pm$. The analysis is based on a data sample corresponding to an integrated luminosity of $\int \mathcal{L}\,dt \approx 6.0\,\mathrm{fb}^{-1}$. We measure the four $\Lambda_b^0\pi^\pm$ resonant states masses to be:

$$\begin{aligned} m(\Sigma_b^+) &= 5811.2^{+0.9}_{-0.8}\,(\mathrm{stat}) \pm 1.7\,(\mathrm{syst})\,\mathrm{MeV}/c^2 \\ m(\Sigma_b^-) &= 5815.5^{+0.6}_{-0.5}\,(\mathrm{stat}) \pm 1.7\,(\mathrm{syst})\,\mathrm{MeV}/c^2 \\ m(\Sigma_b^{*+}) &= 5832.0 \pm 0.7\,(\mathrm{stat}) \pm 1.8\,(\mathrm{syst})\,\mathrm{MeV}/c^2 \\ m(\Sigma_b^{*-}) &= 5835.0 \pm 0.6\,(\mathrm{stat}) \pm 1.8\,(\mathrm{syst})\,\mathrm{MeV}/c^2 \end{aligned}$$

We report the first measurement of isospin mass splittings for the $J^P = \frac{1}{2}^+$ and $J^P = \frac{3}{2}^+$ isospin multiplets of $\Sigma_b^{(*)}$ bottom baryons to be:

$$\begin{aligned} m(\Sigma_b^+) - m(\Sigma_b^-) &= -4.2^{+1.1}_{-0.9}\,(\mathrm{stat})^{+0.07}_{-0.09}\,(\mathrm{syst})\,\mathrm{MeV}/c^2 \\ m(\Sigma_b^{*+}) - m(\Sigma_b^{*-}) &= -3.0 \pm 0.9\,(\mathrm{stat})^{+0.12}_{-0.13}\,(\mathrm{syst})\,\mathrm{MeV}/c^2 \end{aligned}$$

We also report the first measurement of the widths of these states:

$$\begin{aligned} \Gamma(\Sigma_b^+) &= 9.2^{+3.8}_{-2.9}\,(\mathrm{stat})^{+1.0}_{-1.1}\,(\mathrm{syst})\,\mathrm{MeV}/c^2 \\ \Gamma(\Sigma_b^-) &= 4.3^{+3.1}_{-2.1}\,(\mathrm{stat})^{+1.0}_{-1.1}\,(\mathrm{syst})\,\mathrm{MeV}/c^2 \\ \Gamma(\Sigma_b^{*+}) &= 10.4^{+2.7}_{-2.2}\,(\mathrm{stat})^{+0.8}_{-1.2}\,(\mathrm{syst})\,\mathrm{MeV}/c^2 \\ \Gamma(\Sigma_b^{*-}) &= 6.4^{+2.2}_{-1.8}\,(\mathrm{stat})^{+0.7}_{-1.1}\,(\mathrm{syst})\,\mathrm{MeV}/c^2 \end{aligned}$$

I. INTRODUCTION

The heavy baryons with a single heavy quark are the helium atoms of QCD with nucleus as a heavy quark Q and two orbiting electrons as a light diquark q_1q_2. The heavy quark in the baryon may be used as a probe of a confinement which at least will allow us to study a non-perturbative QCD somewhat deeper than we do it with light baryons.

The remarkable achievements in a theory of heavy quark hadrons have been made when it was realized that a single heavy quark Q with the mass $m_Q \gg \Lambda_{\rm QCD}$ in the heavy hadron H_Q can be considered as an "essentially static color source in the hadrons's rest frame" [1]. Thence the light diquark properties of a charm baryon $\Lambda_c^+\,(\Sigma_c)$ and its bottom partner $\Lambda_b^0\,(\Sigma_b)$ can be related by an approximate $SU(2)$ symmetry due to $c \leftrightarrow b$ quark exchange. Another symmetry emerges because the spin S_Q degree of freedom decouples from the gluon field and S_Q generates another $SU(2)$ symmetry of a light degrees of freedom in the effective field theory of the heavy hadron H_Q. The models having these Heavy Quark Symmetries (HQS) are grouped as Heavy Quark Effective Theories (HQET). Some of the further original works on HQET can be found in [2],[3],[4],[5] while the comprehensive reviews on the subject with the references therein are in [6],[7].

As the spin S_{qq} of a diquark (plus a gluon field) and the one S_Q of a heavy quark are decoupled in HQET and serve as good quantum numbers, heavy baryons can be assigned the quantum numbers S_Q, m_Q, S_{qq}, m_{qq}. Therefore the total spins of the S- wave ($l_{qq} = 0$, no orbital excitation) baryon multiplets can be expressed as a simple sum $J = S_Q + S_{qq}$. Then the singlet Λ_b^0 baryon with quark content $b[ud]$ according to HQET has spin of the heavy quark to be $S_b = \frac{1}{2}^+$ and its flavor antisymmetric $[ud]$- di-quark has a spin of $S_{[ud]} = 0$. At these conditions the b- quark and $[ud]$ make lowest-lying singlet ground state $J^P = \frac{1}{2}^+$. The partner of the Λ_b^0 baryon in the strange quark sector is the famous Λ^0.

The other two states Σ_b, Σ_b^* with the quark content $b\{q_1q_2\}$, a heavy quark spin $S_b = \frac{1}{2}^+$ and a spin of the flavor symmetric di-quark $S_{\{q_1q_2\}} = 1^+$ constitute two isospin $I = 1$ triplets with the total spin $J^P = \frac{1}{2}^+$ and $J^P = \frac{3}{2}^+$. These states are the lowest-lying S- wave states which can decay to the singlet Λ_b^0 via strong processes involving soft pion emissions provided sufficient phase space is available for a given mode (see Fig. 1). According to an established nomenclature Σ_b, Σ_b^* are the resonance states. The partners of $\Sigma_b^{(*)}$ states in the strange quark sector are $\Sigma^{(*)}$ resonances though one has to mention that [8] the $J^P = \frac{1}{2}^+$ states Σ are light enough to decay only weakly or radiatively and only $J^P = \frac{3}{2}^+$ states $\Sigma(1385)$ do decay strongly via $\Lambda^0\pi$ mode.

Some recent HQET calculations for bottom baryons are done in [9],[10],[11], [12],[13]. The mass spectra of single heavy quark baryons with HQET calculated in combined expansions in $1/m_Q$, $1/N_c$ are presented in [14],[15],[16].

In potential quark model the mass differences like $\Sigma_Q - \Lambda_Q$, $\Sigma_Q^* - \Sigma_Q$ are accounted largely by hyperfine splittings, hence the mass differences scale as $1/m_Q$. Some of recent predictions based on potential quark models have been published by [17], [18],[19], [20],[21],[22],[23], [24],[25],[26]. The authors of [27] (see references herein) employ the constituent quark model and solve the three-quark problem exactly.

The interesting QCD string quark model is used by in [28],[29] to calculate masses of the heavy baryons.

There are striking regularities in the masses and mass differences of known hadrons. Some of these regularities can be understood from known general properties of the interactions of quarks without a need to specify the explicit form of the Hamiltonian. Following this minimalist approach the authors [30],[31],[32] use semi-empirical mass formulas to predict the spectrum of heavy c- and b- baryons.

The non-perturbative formalism of QCD sum rules [33],[34] has been further developed by B. L. Ioffe [35] for baryons. Inspired by the recent experimental results (see e.g. [36]) X. Liu *et al.* [37] (see also a trail of references herein) applied the QCD sum rules approach in HQET. Another method within QCD sum rules have been used by [38] (see also references herein) to calculate mass spectra of the heavy baryons Λ_Q and Σ_Q.

The lattice non-relativistic QCD (NRQCD) calculations for bottom baryons have been quite successful in [39],[40] though the statistical and systematic Al uncertainties are typically large and exceed the errors of the experimental measurements.

The recent comprehensive review on experimental and theoretical status of baryon spectroscopy can be found in [41] with many useful references therein.

Few of the theoretical predictions on Λ_b^0 and Σ_b masses from the sources discussed above are shown in the Table I.

The mass splitting between members of $I = 1$ isospin triplets $\Sigma_b^{(*)}$ is expected to be determined by the electromagnetic interactions between light quarks, due to an intrinsic mass difference between the light u and d quarks and other non-perturbative QCD contributions, please see [42] and references therein. As the d- quark is heavier than the u- partner, the $\Sigma_b^{(*)-}$ states with $b\{dd\}$ quarks are expected to be heavier than the corresponding $\Sigma_b^{(*)+}$ ones with $b\{uu\}$ quark content. The experimental measurement of this value could provide an additional insight into interplay between electromagnetic and strong contributions leading to the mass differences within baryon isospin triplets. The

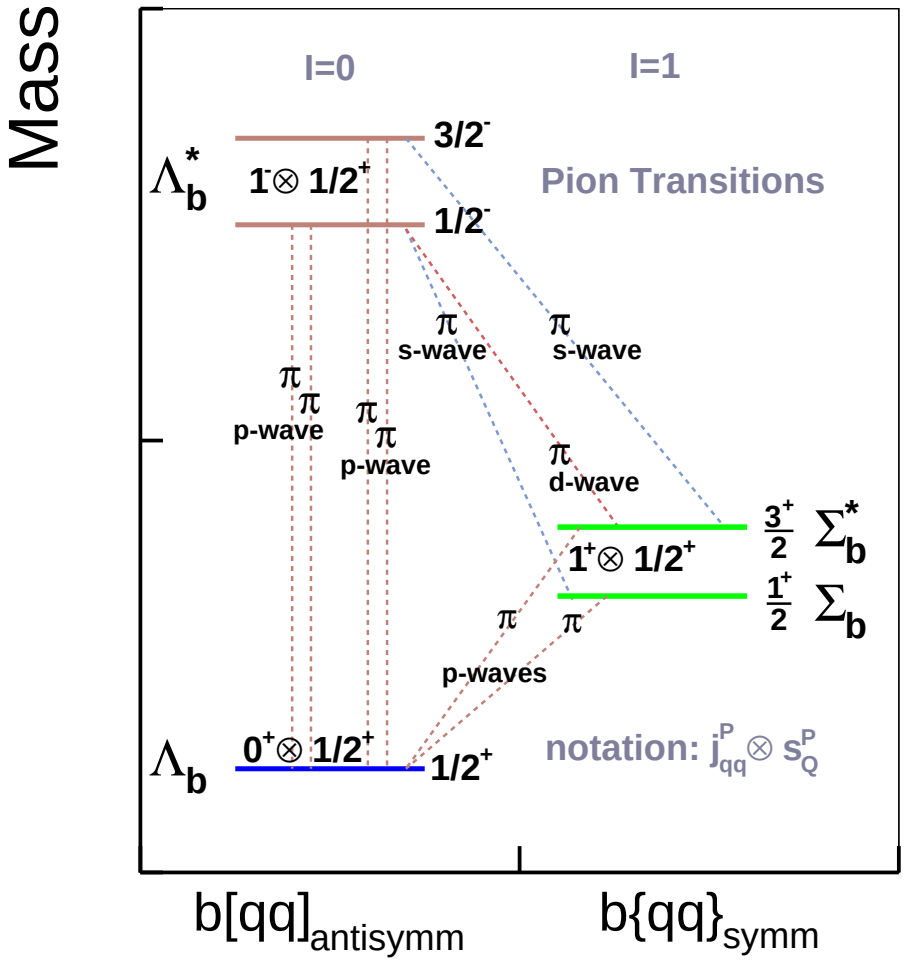

FIG. 1: The pion transitions of low lying S-wave $\Sigma_b^{(*)}$ states and a first orbital P-wave excitations Λ_b^{*0}. The shown resonance states undergo the strong decays to the lowest lying singlet Λ_b^0 provided the necessary phase space volume available.

available for $\Sigma_b^{(*)}$ baryons quark model predictions [43], [44], [45], [46] are listed in the Table II.

The description of the strong decays of baryon resonances is a difficult theoretical task [19]. Few of available theoretical predictions on natural widths are arranged into the Table III.

A. Motivation of the Experimental Study

This study succeeds the CDF publication [36] on a discovery of $\Sigma_b^{(*)}$ states.

We intend to confirm the observation of those states using a larger data-sample, address critical points [41] of the published [36] analysis and proceed with measurements of properties of $\Sigma_b^{(*)}$ resonances.

The scope of the presented below analysis includes the items:

- Use all data collected by CDF comprising a total luminosity $\int \mathcal{L}\, dt = 6\,\mathrm{fb}^{-1}$.
- Perform fits of $\Sigma_b^{(*)}$ Q- value spectra for every isospin partner state, $\Sigma_b^{(*)+}$ and $\Sigma_b^{(*)-}$, independently and without constrain on the mass difference $\Delta = M(\Sigma_b^*) - M(\Sigma_b)$.

Reference	$M(\Lambda_b^0)$, MeV/c^2	$M(\Sigma_b, \frac{1}{2}^+)$, MeV/$c^2$	Q, MeV/c^2	$M(\Sigma_b^*, \frac{3}{2}^+)$, MeV/$c^2$	Q^*, MeV/c^2
Faustov [11, 12]	5622	5805	43.4	5834	72.4
Karliner [23]	5619.7 [61] (CDF II)	5814	~ 54.7	5836	~ 76.7
Narodetskii [28]	5619.7 [61] (CDF II)	5808 [36] (CDF II)	~ 48.7	5833	73.7
Garcilazo [27]	5624	5789	24.4	5844	79.4
Zhang [38]	5690 ± 130	5730 ± 210	-100 ± 247	5810 ± 190	-20 ± 230
Mathur [39]	$5672 \pm ^{+108}_{-110}$	–	53.4^{+37}_{-36}	–	$(\Sigma_b^* - \Sigma_b)$
$\beta = 2.3$				–	24^{+13}_{-12}
$\Sigma_b^{(*)-}$ [36] (CDF II)	5619.7 ± 1.5	$5815.2^{+2.0}_{-2.0}$	$55.9^{+1.0}_{-1.0}$	$5836.4^{+2.7}_{-2.6}$	$Q^{*\pm} - Q^{\pm} =$
$\Sigma_b^{(*)+}$ [36] (CDF II)	5619.7 ± 1.5	$5807.8^{+2.6}_{-2.8}$	$48.5^{+2.0}_{-2.2}$	$5829.09^{+2.3}_{-2.5}$	$= 21.2^{+2.0}_{-1.9}$

TABLE I: The mass predictions for $\Sigma_b^{(*)}$ states. The Q- value is defined as $Q = M(\Sigma_b^{(*)}) - M(\Lambda_b^0) - m(\pi^{\pm})_{PDG}$. The CDF II results [36] are shown in bottom lines. Some models use the CDF II measured Λ_b^0 mass [61] as an input parameter.

Reference	$\Sigma_b^+ - \Sigma_b^-$ MeV/c^2	$\Sigma_b^{*+} - \Sigma_b^{*-}$ MeV/c^2
Chan [43]	-6.12	-5.82
Lichtenberg [44]	-7.1	-6.5
Capstick [45]	-5.6	-5.4
Varga [46]	-2.51	n/a

TABLE II: The predictions on isospin mass splittings for $\Sigma_b^{(*)}$ states.

- Leave background shapes floating in the fits. Thus we avoid the systematic uncertainty coming from Monte-Carlo models.
- Confirm the observed signals with the dramatically increased significance.
- Produce the direct mass difference measurements with smaller statistic and systematic uncertainties.
- Measure intrinsic natural widths of both $J^P = \frac{3}{2}^+$ and $J^P = \frac{1}{2}^+$ states.
- Based on new mass measurements quote the isospin mass splitting for Σ_b and Σ_b^* isospin $I = 1$ triplets.

With the experimental program outlined above we will provide the next input to the theoretical community initiating the new round of heavy baryon calculations and challenge the model makers with somewhat newer tasks like e.g. natural width estimates.

II. CDF II DETECTOR AND TRIGGER

The component of the CDF II detector [50] most relevant for this analysis is the tracking system. The tracking system is embedded into a uniform axial 1.4 T field generated by a super-conducting solenoidal magnet. The inner tracking volume up to a radius of 22 cm is filled with 6 layers of double-sided silicon micro-strip detectors, the *Silicon*

Reference	$\Gamma(\Sigma_b, \frac{1}{2}^+)$, MeV/$c^2$	$\Gamma(\Sigma_b^*, \frac{3}{2}^+)$, MeV/$c^2$
Körner [47]	~ 8	~ 15
Guo [48]	$(6.73 - 13.45)$	$(10.00 - 17.74)$
C.-W. Hwang [49], $\Sigma_b^{(*)+}$	4.35	8.50
C.-W. Hwang [49], $\Sigma_b^{(*)-}$	5.77	10.44

TABLE III: The predictions on natural widths for $\Sigma_b^{(*)}$ states.

Vertex Detector (SVX II), and the *Intermediate Silicon Layers* (ISL) [51]. An additional layer of single-sided silicon, the *Layer00* (L00) [51], is mounted directly on the beam-pipe at a radius of 1.5 cm, providing an excellent resolution of the track impact parameter d_0, defined in the transverse plane. The volume between the radii of 40 cm and 137 cm is instrumented with a drift chamber, the *Central Outer Tracker* (COT) [52].

A three-tiered trigger system is used for the online event selection. The trigger components important for this analysis are the *eXtremely Fast Tracker* (XFT) [53], which, at Level 1 finds tracks with $p_T > 1.5\,\mathrm{GeV}/c$ using hits in four axial super-layers of the COT. The Level 2 *Silicon Vertex Trigger* (SVT) [54] combines the input from XFT with $r-\phi$ hits from the SVX II detector and recognizes tracks using a large look-up table of hit patterns. The fine offline-like impact parameter resolution of 30 μm allows the selection of long-lived particles at the trigger level.

The events are selected by the *Displaced track* trigger, which selects events that contain track pairs with a transverse momentum of each track to be above 2 GeV/c and an impact parameter to be within the range, 120 $\mu\mathrm{m} < |d_0| < 1$ mm. These tracks are referred to as "trigger tracks". The *Displaced track* trigger ensures an enriched sample on b-hadron decays.

III. DATA SAMPLE & EVENT SELECTION

This analysis is based on an integrated luminosity of 6.0 fb^{-1} collected with the CDF II detector between March 2002 and February 2010. We study decays in the exclusively full reconstructed decay channel, $\Sigma_b^{(*)\pm} \to \Lambda_b^0\pi^\pm_{soft}$, $\Lambda_b^0 \to \Lambda_c^+\pi_b^-$, $\Lambda_c^+ \to pK^-\pi^+$ [63].

The analysis begins with the reconstruction of the $\Lambda_c^+ \to pK^-\pi^+$ decay by fitting three tracks to a common vertex. Then, the $\Lambda_b^0 \to \Lambda_c^+\pi_b^-$ candidate is subjected to a single π_b^--track vertex fit with the contributing Λ_c^+ candidate constrained to its PDG [8] mass. At this stage of the reconstruction at least two tracks within p, K^-, π^+, π_b^- are demanded to be SVT tracks.

Finally, the Λ_b^0 candidate is combined with a soft pion track and again the $\Sigma_b^{(*)\pm} \to \Lambda_b^0\pi^\pm_{soft}$ candidate is subjected to a single track vertex fit. The signal analysis is performed with the Q-value distributions, $Q = m(\Lambda_b^0\pi^\pm_{soft}) - m(\Lambda_b^0) - m(\pi^\pm)_{\mathrm{PDG}}$ where the Λ_b^0 candidate's resolution and most of the systematic uncertainties are canceled.

A. Optimization Analysis Requirements

The choice of analysis cuts to identify $\Lambda_b^0 \to \Lambda_c^+\pi^-$ candidates has been made using the optimization based on the experimental data only. The figure of merit, $S/\sqrt{S+B}$ used during the optimization of cuts set a relation between the signal S and the background B under the signal both yielded by fits of an invariant mass $m(\Lambda_c^+\pi^-)$ spectrum.

Table IV summarizes the Λ_b^0 analysis cuts after the optimization. Figure 2 shows the Λ_b^0 signal after applying the optimized cuts. The world record yield of the Λ_b^0 signal in CDF detector amounts to $\sim$ 16300 candidates with the integrated luminosity of 6 fb^{-1} while the S/B is kept of ≈ 1.8.

The random combinations of optimized Λ_b^0 candidates with $\pi^\pm_{soft}$ tracks constitute the dominating background under $\Sigma_b^{(*)\pm} \to \Lambda_b^0\pi^\pm_{soft}$ signals [36] as a number of soft tracks are produced in a b-quark hadronization and in the underlying event. The tracking quality criteria and the analysis cuts applied to the soft pion track are arranged in the Table IV as well.

IV. FITTER DESCRIPTION

The signals of $\Sigma_b^\pm$ and $\Sigma_b^{*\pm}$ are reconstructed as two peaks in a Q- value spectrum, $Q = m(\Lambda_b^0\pi^\pm_{soft}) - m(\Lambda_b^0) - m(\pi^\pm)$.

Since both states are produced in the vicinity of a threshold at $Q \sim 50\,\mathrm{MeV}/c^2$ and $Q \sim 70\,\mathrm{MeV}/c^2$, the signal shape is modeled with a non-relativistic Breit-Wigner function, modified to account for the pion emitted in a P-wave (see Sec. IV A). The Breit-Wigner function is further convoluted with the detector resolution described by two Gaussians with their widths σ_1, σ_2 and weights g, $(1-g)$ calculated from Monte-Carlo simulation.

A. P-Wave Modified Breit-Wigner Function

The soft pion in strong decay modes is emitted in a P-wave. We follow an approach proposed by J. D. Jackson [55, 56] and applied to strange resonance studies. The approach has been employed also by CLEO Collaboration in their

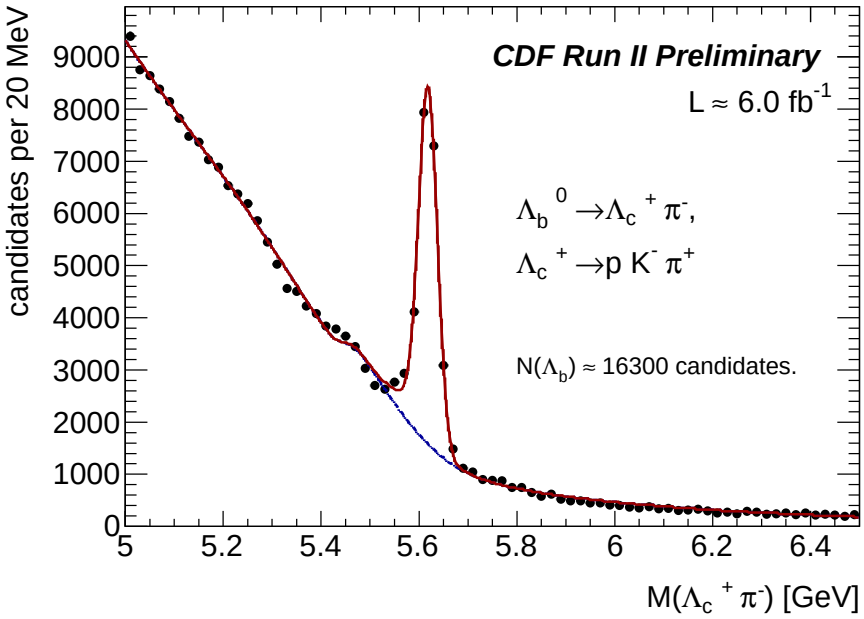

FIG. 2: Λ_b^0 signal reconstructed using the total statistics of $\int \mathcal{L}\, dt = 6\,\mathrm{fb}^{-1}$.

analyses on Σ_c charm baryons [57, 58]. The signal shape reconstructed in P-wave modes is asymmetrical and biased towards the higher masses due to a well known P- wave factor. To correct out the effect the natural width Γ in the Breit-Wigner function is factorized with a phenomenological term $(\frac{p^*_\pi}{p^{*0}_\pi})^{2\cdot L+1}$, where p^*_π, p^{*0}_π are the momenta of an emitted in a $\Sigma_b^{(*)}$ rest frame soft pion π off and at the resonance pole mass value.

That is for our case, $L = 1$, (see [8] for further kinematic calculations) thence

$$\Gamma(Q; Q_0, \Gamma_0) = \Gamma_0 \cdot \left(\frac{p^*_\pi}{p^{*0}_\pi}\right)^3 ,$$

where Q_0 is a mass at the pole, and Γ_0 is a corrected width, both are floating fit parameters.

B. Background Model

We use a phenomenological model for the background described by a second order polynomial modulated with a threshold `sqrt`- factor, specifically

$$\mathcal{BGR}(Q; thr, C, b_1, b_2) \;=\; \sqrt{(Q+m_\pi)^2 \;-\; thr^2}\cdot \left(C \;+ b_1 \cdot\; Q + b_2 \cdot\; (2\cdot Q^2 \;- 1)\right) ,$$

where C, b_1 and b_2 are the polynomial (Chebyshev) coefficients and thr is a threshold to be a mass of a pion. We keep thr fixed to $thr = 0.140\,\mathrm{GeV}/c^2$. As the fitter is expected to run with extended likelihood, one of the polynomial coefficients, b_2 will also be fixed. The term $\sqrt{(Q+m_\pi)^2 \;-\; thr^2}$ has been used by many experiments (see for example CLEO analysis [59]) to describe a combinatorial background of 2-body decays near the threshold when the signals are reconstructed in a mass difference spectra.

V. SIGNIFICANCE

The significance of the observed signals is tested against several null hypothesis using the log-ratio of the minima likelihoods, $\mathcal{L}_1/\mathcal{L}_0$, reached by the fitter for our base line fit model hypothesis, –log $\mathcal{L}_1$ and for a particular null

Tracks or candidate	Cut Quantity	value
p, K, $\pi^{\pm}$ from $\Lambda_b^0 \to \Lambda_c^+ \pi_b^-$, $\Lambda_c^+ \to pK^-\pi^+$	N(COT–stereo) hits	≥ 10
	N(COT–axial) hits	≥ 10
	N(r–ϕ) SVX II hits	≥ 3
	$\lvert d_0 \rvert$	$< 0.1\,\mathrm{cm}$
	p_T	$> 400\,\mathrm{MeV}/c$
$\Lambda_b^0 \to \Lambda_c^+ \pi_b^-$	$ct(\Lambda_b^0)$	$> 200\,\mu\mathrm{m}$
	$ct(\Lambda_b^0)/\sigma_{ct}$	> 12.0
	$\lvert d_0 \rvert(\Lambda_b^0)$	$< 80\,\mu\mathrm{m}$
	$ct(\Lambda_c^+ \leftarrow \Lambda_b^0)$	$> -150\,\mu\mathrm{m}$
	$ct(\Lambda_c^+ \leftarrow \Lambda_b^0)$	$< 250\,\mu\mathrm{m}$
	$p_T(\pi_b^-)$	$> 1.5\,\mathrm{GeV}/c$
	$p_T(\Lambda_b^0)$	$> 4.0\,\mathrm{GeV}/c$
	$\lvert m(\Lambda_c^+\pi^-) - m(\Lambda_b^0) \rvert$	$< 3 \cdot 19.22\,\mathrm{MeV}/c^2$, $\pm 3\sigma$
		$\mathrm{m}(\Lambda_b^0) = 5619.15\,\mathrm{MeV}/c^2$
	Prob(χ^2_{3D}) of Λ_b^0 vertex fit	> 0.0001
$\pi^{\pm}_{soft}$ from $\Sigma_b^{*\pm}$	N(COT–stereo) hits	no hits found
	N(COT–axial) hits	no hits found
	N(r–ϕ) SVX II hits	≥ 4
	OR	
	Any of COT, N(COT–stereo) **or** N(COT–axial), hits	≥ 1
	N(r–ϕ) SVX II hits	≥ 3
	$\lvert d_0 \rvert$	$< 0.1\,\mathrm{cm}$
	p_T	$> 200\,\mathrm{MeV}/c$
$\Sigma_b^{*\pm} \to \Lambda_b^0 \pi^{\pm}_{soft}$	$p_T(\Sigma_b^{(*)})$	$> 4.0\,\mathrm{GeV}/c$
	$\lvert d_0/\sigma_{d_0} \rvert(\pi_{soft})$	< 3.0
	$p_T(\pi_{soft})$	$< p_T(\pi_b^-)$

TABLE IV: Final selection cuts after optimization. The track quality requirements for nominal tracks with $p_T > 400\,\mathrm{MeV}/c$ and for soft tracks with $p_T > 200\,\mathrm{MeV}/c$ are shown. ct is a proper life-time, d_0 is an impact parameter of a candidate defined in a transverse plane.

hypothesis, –log $\mathcal{L}_0$ our default base line one is going to be tested against.

$$-2 \cdot \log \frac{\mathcal{L}_0}{\mathcal{L}_1} = -2 \cdot \Delta(log\mathcal{L})$$

We interpret the above written log-ratio as a χ^2 of the null hypothesis spectrum to fluctuate to our base signal one with a number of degrees of freedom equal to the difference in the number of floating parameters between both hypotheses. We consider the next null hypotheses to estimate significances of the two-peak signal structure or individual peaks of observed $\Sigma_b^{(*)\pm}$ states, to be specific

- Any single peak instead of the two ones is observed, the null hypotheses is a single peak p.d.f on top of the same polynomial background as in the base model: the single peak spectrum fluctuates to two peaks with $\Delta\mathrm{NDF} = 3$. The width of the single peak is floating, within $\Gamma_0 \in (0.001, 0.070)\,\mathrm{GeV}/c^2$ as well as its position, $Q_0 \in (0.003, 0.210)\,\mathrm{GeV}/c^2$. We expect that this test is going to be the most critical one.

- The signal Σ_b^* is observed but the Σ_b has been missed. The background at the left fluctuates to the peak of Σ_b with $\Delta\mathrm{NDF} = 4$. We impose a loose requirement on an existence of the second peak, Σ_b^*, i.e. we fix only the width of Σ_b^* to the expected theoretical value of $12\,\mathrm{MeV}/c^2$ but let the fitter to find and fit the Σ_b^* position which is again floating, within $Q_0 \in (0.003, 0.210)\,\mathrm{GeV}/c^2$.

- The signal Σ_b is observed but the Σ_b^* has been missed. The background at the right fluctuates to the peak of Σ_b^* with $\Delta\mathrm{NDF} = 4$. We impose a loose requirement on an existence of the first peak, Σ_b, i.e. we fix only the width of Σ_b to the expected theoretical value of $7\,\mathrm{MeV}/c^2$ but let the fitter to find and fit the Σ_b position which is again floating, within $Q_0 \in (0.003, 0.210)\,\mathrm{GeV}/c^2$.

Null Hypo.	$-2\cdot\Delta(log\mathcal{L})$	ΔNDF	Prob(χ^2)	N_σ	Comment
Any single peak	$-2\cdot(-32)$	3	$\approx 8.2\cdot10^{-14}$	7.5	w.r.t. double pk.
No Σ_b^-, with Σ_b^{*-}	$-2\cdot(-35)$	4	$\approx 2.3\cdot10^{-14}$	7.6	w.r.t. double pk. $\Gamma_{02}=12\,\mathrm{MeV}/c^2$
No Σ_b^{*-}, with Σ_b^-	$-2\cdot(-57)$	4	$\approx 1.0\cdot10^{-23}$	10.0	w.r.t. double pk. $\Gamma_{01}=7\,\mathrm{MeV}/c^2$
No signals	$-2\cdot(-55)$	3	$\approx 1.1\cdot10^{-23}$	10.0	w.r.t. single pk.
No signals	$-2\cdot(-87)$	6	$\approx 6.4\cdot10^{-35}$	12.3	w.r.t. double pk.

TABLE V: Tests of the baseline $\Sigma_b^{(*)-}$ fit results against several null hypothesis. Robust significance above Gaussian $7.0\,\sigma$ is found.

Null Hypo.	$-2\cdot\Delta(log\mathcal{L})$	ΔNDF	Prob(χ^2)	N_σ	Comment
Any single peak	$-2\cdot(-30)$	3	$\approx 5.9\cdot10^{-13}$	7.2	w.r.t. double pk.
No Σ_b^+, with Σ_b^{*+}	$-2\cdot(-33)$	4	$\approx 1.6\cdot10^{-13}$	7.4	w.r.t. double pk. $\Gamma_{02}=12\,\mathrm{MeV}/c^2$
No Σ_b^{*+}, with Σ_b^+	$-2\cdot(-84)$	4	$\approx 2.8\cdot10^{-35}$	12.4	w.r.t. double pk. $\Gamma_{01}=7\,\mathrm{MeV}/c^2$
No signals	$-2\cdot(-79)$	3	$\approx 4.9\cdot10^{-34}$	12.2	w.r.t. single pk.
No signals	$-2\cdot(-109)$	6	$\approx 2.8\cdot10^{-44}$	14.0	w.r.t. double pk.

TABLE VI: Tests of the baseline $\Sigma_b^{(*)+}$ fit results against several null hypothesis. Robust significance above Gaussian $7.0\,\sigma$ is found.

- Any single peak is observed, the null hypotheses is our base background model: the background fluctuates to this single peak with $\Delta\mathrm{NDF}=3$. This test should determine the significance of a single peak model w.r.t. to a pure background.
- Neither Σ_b and Σ_b^* are observed, the null hypotheses is our base line background model: the background fluctuates to two peaks with $\Delta\mathrm{NDF}=6$. This test is expected to be the least critical one.

Tables V and VI summarize the results of these tests. For every null hypothesis tested the significance is above 7.0σ in Gaussian terms.

VI. SYSTEMATIC UNCERTAINTIES

Systematic uncertainties in this analysis come from three sources:

- Fit bias: we have tested a performance of our unbinned likelihood fitter running it with 10000 statistical trials, the fitter behaves stable, though reveals a small bias for a width parameter, Γ_0. We account this bias as a systematic uncertainty.
- Uncertainty on the momentum scale.
- Assumptions made about the fitter. These ones include the following:
  - Fixed parameters on the fitter describing the resolution of the detector. This is the dominant contribution to the total systematic uncertainty on the width measurements.
  - The model describing the background.

The effect on the $\Sigma_b^{(*)}$ pole Q_0-values uncertainty due to momentum scale is estimated by comparing the differences of the Q_0-values between CDF and the *Particle Data Group* (PDG) [8] for several other low-energy resonances ($\Sigma_c^{++} \to \Lambda_c^+\pi^+$, $\Sigma_c^0 \to \Lambda_c^+\pi^-$, $\Lambda_c^{*+} \to \Lambda_c^+\pi^+\pi^-$ and $D^{*+} \to D^0\pi^+$). We plot the difference between the CDF and PDG Q_0-values as a function of the Q_0-value of the decay, and fit the graph to a linear function. The value of the function at the measured $\Sigma_b^{(*)}$ pole Q_0 incremented with the linear fit error conservatively result the sought piece of the uncertainty.

Following method used by [60] the D^{*+} signal peak in a mass difference, $m(D^{*+}) - m(D^0)$ distribution has been reconstructed in several bins on the soft pion transverse momentum $p_T(\pi_{soft})$. The signal has been subjected to a fit with the sum of a Breit-Wigner function convoluted with a double Gaussian function to describe the detector resolution and of a background modeled by a product of an exponential and a power functions. For every of $p_T(\pi_{soft})$ bins the fits find the D^{*+} natural widths to be below than $0.2\,\mathrm{MeV}/c^2$. Furthermore the D^{*+} natural width, $0.096\pm0.022\,\mathrm{MeV}/c^2$ [8] is much smaller than a CDF II tracking resolution. Thence the value of $0.2\,\mathrm{MeV}/c^2$ is assigned as a systematic uncertainty of the natural width due to a momentum scale of CDF tracker, see also [60] .

The systematic uncertainties related to the assumptions made about the fitter were evaluated by generating many statistical trials with Q- value spectra distributed according to the signal model but with the changed parameter while fitting the spectra with the same parameter set as in data.

The uncertainty due to the systematic variation of the parameters describing the resolution is the dominant contribution to the systematic uncertainty on the widths. In order to estimate a systematic uncertainty from this source, we select the range of variation of these parameters according to the observed differences between data and Monte-Carlo in the decay $D^{*\pm} \to D^0\pi^\pm$. Figure 3 shows these comparison between data and Monte-Carlo.

The systematic uncertainties are summarized in the Table VII.

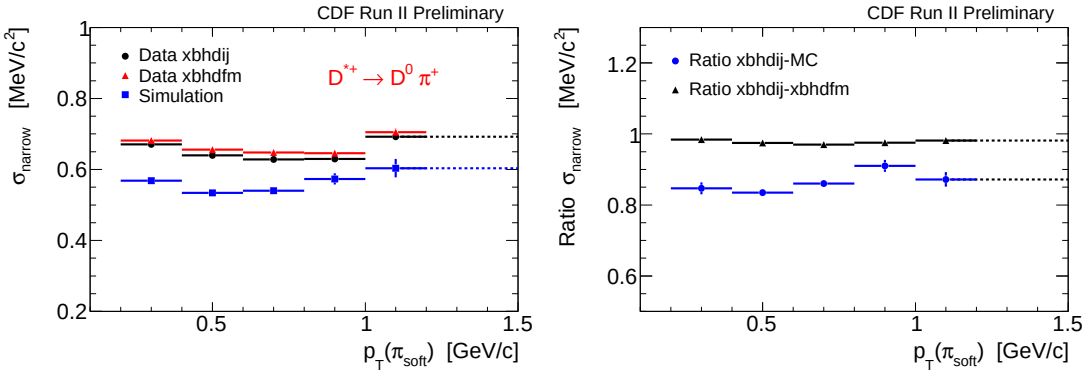

FIG. 3: Left hand side plot shows the resolution of the decay $D^{*+} \to D^0\pi^+_{soft}$ for two data samples taken at different luminosities and for a Monte-Carlo sample. The right hand side plot shows the resolution ratio between the two different data samples and between data and Monte-Carlo as well. Note that the resolution is stable for data taken at different times.

VII. RESULTS

Figure 4 shows the $\Sigma_b^{(*)\pm}$ Q-value distributions with the projection of the unbinned fits superimposed. The measurement results are arranged in a Table VIII. From the measured $\Sigma_b^{(*)\pm}$ Q-values we extract the absolute masses using the PDG value of the $\pi^\pm$ mass and the best CDF mass measurement for Λ_b^0, which is $m(\Lambda_b^0) = (5619.7 \pm 1.2\,(\mathrm{stat}) \pm 1.2\,(\mathrm{syst}))\ \mathrm{MeV}/c^2$ [61]. The Λ_b^0 statistical and systematic uncertainties contribute to the systematic error on the $\Sigma_b^{(*)\pm}$ absolute masses.

Using measured Q- values it is straightforward to extract the isospin mass splittings within two isotriplets $J^P = \frac{1}{2}^+$ and $J^P = \frac{3}{2}^+$. For the resulting values, the quoted statistical errors are the corresponding Q- measurements statistical errors added in quadrature. To quote the systematic error, we added in quadrature the uncertainty due to the assumed background, while the other uncertainty sources are correlated and their differences are added in quadrature.

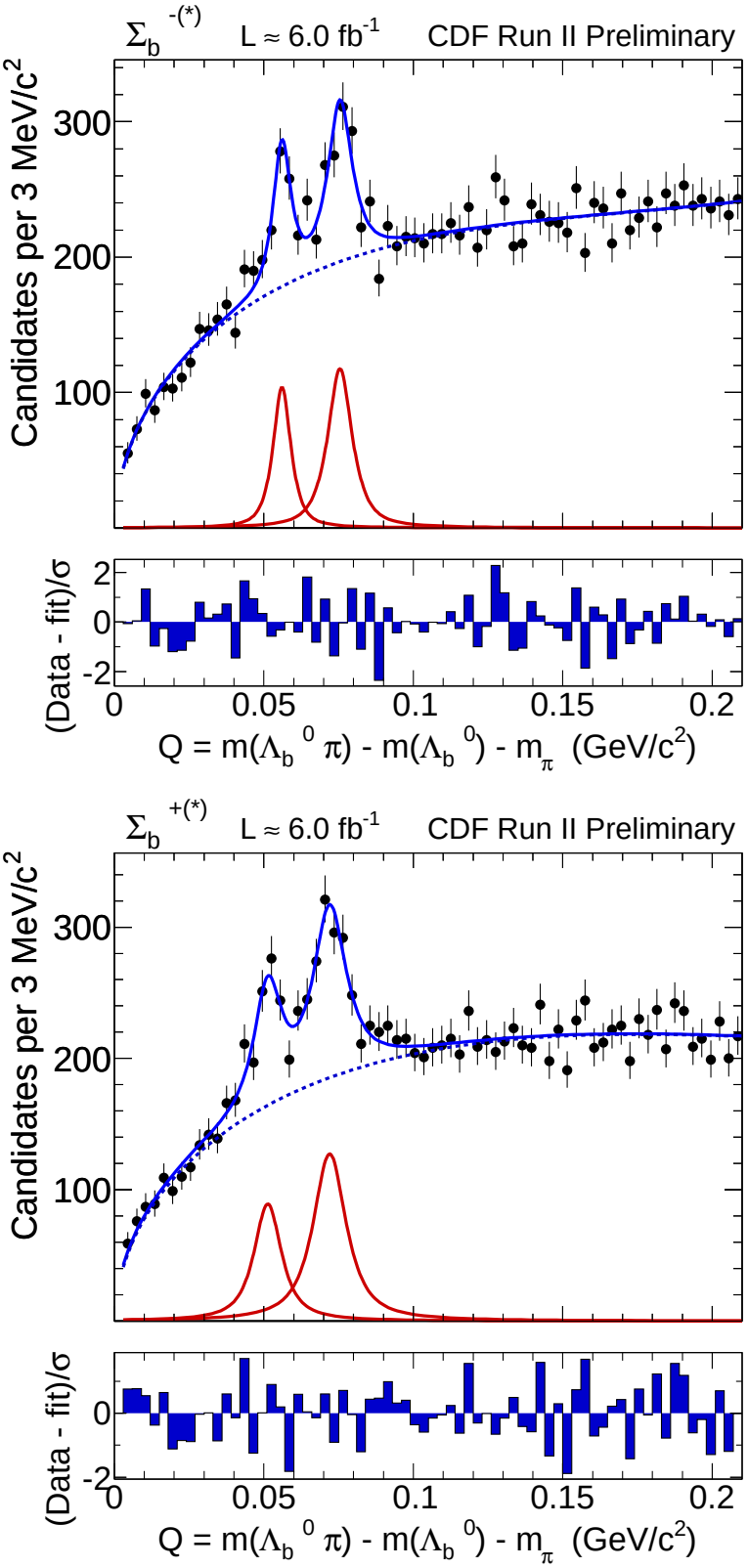

FIG. 4: The Q-value spectra, where $Q = M(\Lambda_b^0\pi^\pm) - M(\Lambda_b^0) - m_{\pi^\pm}$, are shown for $\Sigma_b^{(*)-}$ (upper plot) and for $\Sigma_b^{(*)+}$ (lower plot) candidates with the projection of the corresponding unbinned likelihood fit superimposed on every plot.

Signal Parameter	Mass Scale	Fit Bias	Res.	Back.	Total	%
Σ_b^+ Q, MeV/c^2			0.07	0.05	0.09	0.2
	−0.35		−0.12	−0.05	−0.37	1
Σ_b^+ Γ, MeV/c^2	0.20		0.94	0.40	1.04	11
	−0.20	−0.38	−0.89	−0.40	−1.07	12
Σ_b^+ events			16	9	18	4
			−11	−9	−15	3
Σ_b^- Q, MeV/c^2			0.05	0.04	0.07	0.1
	−0.38		−0.07	−0.04	−0.39	1
Σ_b^- Γ, MeV/c^2	0.20		0.85	0.50	1.01	23
	−0.20	−0.27	−0.87	−0.50	−1.06	25
Σ_b^- events			9	34	35	11
			−8	−34	−35	10
Σ_b^{*+} Q, MeV/c^2			0.06	0.10	0.12	0.2
	−0.52		−0.13	−0.10	−0.55	1
Σ_b^{*+} Γ, MeV/c^2	0.20		0.64	0.50	0.83	8
	−0.20	−0.29	−1.01	−0.50	−1.18	11
Σ_b^{*+} events			7	24	25	3
			−13	−24	−27	4
Σ_b^{*-} Q, MeV/c^2			0.06	0.06	0.08	0.1
	−0.56		−0.08	−0.06	−0.57	1
Σ_b^{*-} Γ, MeV/c^2	0.20		0.65	0.30	0.74	12
	−0.20	−0.23	−0.96	−0.30	−1.05	16
Σ_b^{*-} events			7	28	29	6
			−8	−28	−29	6

TABLE VII: Summary of the systematic errors. For every parameter, the systematic errors associated with the corresponding uncertainty sources are listed in the following order: mass scale, fit procedure, resolution and assumed background. The total systematic error is obtained by adding all the associated errors in quadrature. The last column shows, for every parameter, the % of the total systematic uncertainty with respect the measured value for this parameter.

State	Q-value, MeV/c^2	Absolute Mass, m, MeV/c^2	Natural Width, Γ, MeV/c^2	Yield, num. of cands.
Σ_b^+	$52.0^{+0.9\ +0.09}_{-0.8\ -0.4}$	$5811.2^{+0.9}_{-0.8} \pm 1.7$	$9.2^{+3.8\ +1.0}_{-2.9\ -1.1}$	$468^{+110\ +18}_{-95\ -15}$
Σ_b^-	$56.2^{+0.6\ +0.07}_{-0.5\ -0.4}$	$5815.5^{+0.6}_{-0.5} \pm 1.7$	$4.3^{+3.1\ +1.0}_{-2.1\ -1.1}$	$333^{+93}_{-73} \pm 35$
Σ_b^{*+}	$72.7 \pm 0.7^{+0.12}_{-0.6}$	$5832.0 \pm 0.7 \pm 1.8$	$10.4^{+2.7\ +0.8}_{-2.2\ -1.2}$	$782^{+114\ +25}_{-103\ -27}$
Σ_b^{*-}	$75.7 \pm 0.6^{+0.08}_{-0.6}$	$5835.0 \pm 0.6 \pm 1.8$	$6.4^{+2.2\ +0.7}_{-1.8\ -1.1}$	$522^{+85}_{-76} \pm 29$
	Isospin Mass Splitting, MeV/c^2			
m(Σ_b^+) - m(Σ_b^-)	$-4.2^{+1.1\ +0.07}_{-0.9\ -0.09}$			
m(Σ_b^{*+}) - m(Σ_b^{*-})	$-3.0 \pm 0.9^{+0.12}_{-0.13}$			

TABLE VIII: Summary of the final results. Masses and widths are in MeV/c^2. In all the quoted values the first uncertainty is statistical and the second one is systematic.

VIII. CONCLUSION

In a conclusion, we have measured the $\Sigma_b^{(*)\pm}$ bottom baryons using a sample of ~ 16300 Λ_b^0 candidates identified in $\Lambda_b^0 \to \Lambda_c^+ \pi^-$ mode. The sample corresponds to an integrated luminosity of $6\,\mathrm{fb}^{-1}$.

The first observation of $\Sigma_b^{(*)\pm}$ bottom baryons made by CDF Collaboration [36] has been confirmed with the every individual signal reconstructed at a significance of $\gtrsim 7\sigma$ in Gaussian terms.

The direct mass difference measurements have been found with the statistical precision by a factor of $\gtrsim 2.3$ better w.r.t. to the published [36] numbers and according to the amount of the statistics available. The measurements are in a good agreement with the previously found results [36].

The isospin mass splittings within $I = 1$ triplets Σ_b and Σ_b^* have been extracted for the first time. The precision of the experimental values is as good as the ones quoted by PDG [8] for Σ_c states. The $\Sigma_b^{(*)-}$ states have a higher mass value than their $\Sigma_b^{(*)+}$ partners following [42] a well known pattern of any known isospin multiplet and contrary to their charm partners [8], Σ_c where the supposedly natural order of masses within isotriplets is still violated [62].

The natural widths of both $\Sigma_b^{\pm}$ and $\Sigma_b^{*\pm}$ states have been measured for the first time. The measurements are in a agreement with the theoretical expectations, see the Table III.

Acknowledgments

We thank the Fermilab staff and the technical staffs of the participating institutions for their vital contributions. This work was supported by the U.S. Department of Energy and National Science Foundation; the Italian Istituto Nazionale di Fisica Nucleare; the Ministry of Education, Culture, Sports, Science and Technology of Japan; the Natural Sciences and Engineering Research Council of Canada; the National Science Council of the Republic of China; the Swiss National Science Foundation; the A.P. Sloan Foundation; the Bundesministerium fuer Bildung und Forschung, Germany; the Korean Science and Engineering Foundation and the Korean Research Foundation; the Particle Physics and Astronomy Research Council and the Royal Society, UK; the Russian Foundation for Basic Research; the Comision Interministerial de Ciencia y Tecnologia, Spain; and in part by the European Community's Human Potential Programme under contract HPRN-CT-20002, Probe for New Physics.

[1] N. Isgur and M. B. Wise, Phys. Lett. B **232**, 113 (1989).
[2] N. Isgur and M. B. Wise, Phys. Lett. B **237**, 527 (1990).
[3] N. Isgur and M. B. Wise, Phys. Rev. D **42**, 2388 (1990).
[4] N. Isgur and M. B. Wise, Phys. Rev. Lett. **66**, 1130 (1991).
[5] N. Isgur and M. B. Wise, Nucl. Phys. B **348**, 276 (1991).
[6] M. Neubert, Phys. Rept. **245**, 259 (1994) [arXiv:hep-ph/9306320].
[7] A. V. Manohar and M. B. Wise, Camb. Monogr. Part. Phys. Nucl. Phys. Cosmol. **10**, 1 (2000).
[8] C. Amsler *et al.* [Particle Data Group], Phys. Lett. B **667**, 1 (2008).
[9] C. Albertus, J. E. Amaro, E. Hernandez and J. Nieves, Nucl. Phys. A **740**, 333 (2004) [arXiv:nucl-th/0311100].
[10] D. Ebert, R. N. Faustov, V. O. Galkin and A. P. Martynenko, Phys. Rev. D **66**, 014008 (2002) [arXiv:hep-ph/0201217].
[11] D. Ebert, R. N. Faustov and V. O. Galkin, Phys. Rev. D **72**, 034026 (2005) [arXiv:hep-ph/0504112].
[12] D. Ebert, R. N. Faustov and V. O. Galkin, Phys. Lett. B **659**, 612 (2008) [arXiv:0705.2957 [hep-ph]].
[13] D. Ebert, R. N. Faustov and V. O. Galkin, Phys. Atom. Nucl. **72**, 178 (2009).
[14] E. E. Jenkins, Phys. Rev. D **54**, 4515 (1996) [arXiv:hep-ph/9603449].
[15] E. E. Jenkins, Phys. Rev. D **55**, 10 (1997) [arXiv:hep-ph/9609404].
[16] E. E. Jenkins, Phys. Rev. D **77**, 034012 (2008) [arXiv:0712.0406 [hep-ph]].
[17] S. Gasiorowicz and J. L. Rosner, Am. J. Phys. **49**, 954 (1981).
[18] S. Capstick and N. Isgur, Phys. Rev. D **34**, 2809 (1986).
[19] S. Capstick and W. Roberts, Prog. Part. Nucl. Phys. **45**, S241 (2000) [arXiv:nucl-th/0008028].
[20] J. L. Rosner, Phys. Rev. D **52**, 6461 (1995) [arXiv:hep-ph/9508252].
[21] J. L. Rosner, J. Phys. G **34**, S127 (2007) [arXiv:hep-ph/0609195].
[22] J. L. Rosner, Phys. Rev. D **75**, 013009 (2007) [arXiv:hep-ph/0611207].
[23] M. Karliner and H. J. Lipkin, Phys. Lett. B **660**, 539 (2008) [arXiv:hep-ph/0611306].
[24] M. Karliner, B. Keren-Zur, H. J. Lipkin and J. L. Rosner, arXiv:0708.4027 [hep-ph].
[25] M. Karliner, Nucl. Phys. Proc. Suppl. **187**, 21 (2009) [arXiv:0806.4951 [hep-ph]].
[26] M. Karliner, B. Keren-Zur, H. J. Lipkin and J. L. Rosner, Annals Phys. **324**, 2 (2009) [arXiv:0804.1575 [hep-ph]].
[27] H. Garcilazo, J. Vijande and A. Valcarce, J. Phys. G **34**, 961 (2007) [arXiv:hep-ph/0703257].
[28] I. M. Narodetskii, C. Semay and A. I. Veselov, Eur. Phys. J. C **55**, 403 (2008) [arXiv:0801.4270 [hep-ph]].
[29] R. Y. Kezerashvili, I. M. Narodetskii and A. I. Veselov, Phys. Rev. D **79**, 034003 (2009) [arXiv:0901.0036 [hep-ph]].
[30] R. Roncaglia, A. Dzierba, D. B. Lichtenberg and E. Predazzi, Phys. Rev. D **51**, 1248 (1995) [arXiv:hep-ph/9405392].
[31] R. Roncaglia, D. B. Lichtenberg and E. Predazzi, Phys. Rev. D **52**, 1722 (1995) [arXiv:hep-ph/9502251].
[32] D. B. Lichtenberg, R. Roncaglia and E. Predazzi, Phys. Rev. D **53**, 6678 (1996) [arXiv:hep-ph/9511461].
[33] M. A. Shifman, A. I. Vainshtein and V. I. Zakharov, Nucl. Phys. B **147**, 385 (1979).
[34] M. A. Shifman, A. I. Vainshtein and V. I. Zakharov, Nucl. Phys. B **147**, 448 (1979).
[35] B. L. Ioffe, Nucl. Phys. B **188**, 317 (1981) [Erratum-ibid. B **191**, 591 (1981)].

[36] T. Aaltonen *et al.* [CDF Collaboration], Phys. Rev. Lett. **99**, 202001 (2007) [arXiv:0706.3868 [hep-ex]].
[37] X. Liu, H. X. Chen, Y. R. Liu, A. Hosaka and S. L. Zhu, Phys. Rev. D **77**, 014031 (2008) [arXiv:0710.0123 [hep-ph]].
[38] J. R. Zhang and M. Q. Huang, Phys. Rev. D **77**, 094002 (2008) [arXiv:0805.0479 [hep-ph]].
[39] N. Mathur, R. Lewis and R. M. Woloshyn, Phys. Rev. D **66**, 014502 (2002) [arXiv:hep-ph/0203253].
[40] R. Lewis and R. M. Woloshyn, Phys. Rev. D **79**, 014502 (2009) [arXiv:0806.4783 [hep-lat]].
[41] E. Klempt and J. M. Richard, Rev. Mod. Phys. **82**, 1095 (2010) [arXiv:0901.2055 [hep-ph]].
[42] F. K. Guo, C. Hanhart and U. G. Meissner, JHEP **0809**, 136 (2008) [arXiv:0809.2359 [hep-ph]].
[43] L. H. Chan, Phys. Rev. D **31**, 204 (1985).
[44] W. Y. P. Hwang and D. B. Lichtenberg, Phys. Rev. D **35**, 3526 (1987).
[45] S. Capstick, Phys. Rev. D **36**, 2800 (1987).
[46] K. Varga, M. Genovese, J. M. Richard and B. Silvestre-Brac, Phys. Rev. D **59**, 014012 (1999) [arXiv:hep-ph/9803340].
[47] J. G. Korner, M. Kramer and D. Pirjol, Prog. Part. Nucl. Phys. **33**, 787 (1994) [arXiv:hep-ph/9406359].
[48] X. H. Guo, K. W. Wei and X. H. Wu, Phys. Rev. D **77**, 036003 (2008) [arXiv:0710.1474 [hep-ph]].
[49] C. W. Hwang, Eur. Phys. J. C **50**, 793 (2007) [arXiv:hep-ph/0611221].
[50] Darin E. Acosta *et al.* [CDF Collaboration]. Measurement of the J/ψ Meson and b–hadron Production Cross $p\bar{p}$ Collisions at $\sqrt{s} = 1960$ GeV/c^2. Phys. Rev., D71:032001, 2005, arXiv:hep-ex/0412071.
[51] Christopher S. Hill [On behalf of the CDF Collaboration]. Operational Experience and Performance of the CDF II Silicon Detector. *Nucl. Instrum. Meth.,* A530:1–6, 2004.
[52] Anthony Allen Affolder *et al.* [CDF Collaboration]. CDF Central Outer Tracker. *Nucl. Instrum. Meth.*, A526:249-299, 2004.
[53] Evelyn J. Thomson *et al.* Online Track Processor for the CDF Upgrade. *IEEE Trans. Nucl. Sci.*, 49:1063-1070, 2002.
[54] J. Adelman *et al. Nucl. Instrum. Meth.*, A572:361-364, 2007
[55] J. D. Jackson, Nuovo Cim. **34**, 1644 (1964).
[56] J. D. Jackson, private communication, 11.06.07.
[57] M. Artuso *et al.* [CLEO Collaboration], Phys. Rev. D **65**, 071101 (2002) [arXiv:hep-ex/0110071].
[58] G. Brandenburg *et al.* [CLEO Collaboration], Phys. Rev. Lett. **78**, 2304 (1997).
[59] T.J.V. Bowcock *et al.* [CLEO Collaboration], Phys. Rev. Lett. **62**, 12404 (1989).
[60] A. Abulencia *et al.* [CDF Collaboration], Phys. Rev. D **73**, 051104 (2006) [arXiv:hep-ex/0512069].
[61] D. E. Acosta *et al.* [CDF Collaboration], Phys. Rev. Lett. **96**, 202001 (2006) [arXiv:hep-ex/0508022].
[62] Felix Wick (for the CDF Collaboration), "Charm baryon spectroscopy at CDF", talk at ICHEP 2010, Paris, 22-28 July 2010, to be published in the Proceedings;
see also CDF Collaboration, "Charm Baryon Spectroscopy", public CDF note 10260, August 12, 2010.
[63] Unless otherwise stated all references to the specific charge combination imply the charge conjugate combination as well.